AIChE

R&D NOTE

PARTICLE TECHNOLOGY AND FLUIDIZATION

Evolution of Particle Size Distribution in a Pulsed SiH_4 Plasma Process

Dong-Joo Kim and Kyo-Seon Kim
Dept. of Chemical Engineering, Kangwon National University, Chuncheon, Kangwon-Do 200-701, Korea

DOI 10.1002/aic.11582
Published online September 4, 2008 in Wiley InterScience (www.interscience.wiley.com).

Keywords: pulsed plasmas, particle coagulation, particle charge distribution, particle size distribution, plasma reactor

Introduction

Particles in the size range from a few nm to μm can be generated in plasma processes such as deposition, etching, and sputtering, and they can cause serious problems for the quality of thin films. Particularly, plasma chemical vapor deposition processes are usually carried out under conditions of low pressure to improve the thin-film quality and also to reduce the generation and growth of particles, at the expense of a decrease in deposition rate. For example, amorphous-silicon thin films grow slowly with a deposition rate of 1–3 Å/s.[1,2]

In a pulsed plasma process, one pulse cycle consists of plasma-on with power supply and plasma-off without power supply, and the periods of plasma-on (t_{on}) and -off (t_{off}) are determined by pulse frequency (f_p) and duty ratio ($D = (t_{on})/(t_{on} + t_{off}) \times 100$). During plasma-on, the electrons obtain high energy by the electric field and collide with molecules to form radicals and ions. Just after plasma-off, most of the electrons are consumed quickly by recombination reaction with positive ions and electron-attachment reaction to neutrals within 10s of μs, and during plasma-off there is no further generation of radicals and ions by electron collision.[3–6] Pulse repetition can reduce the concentration of precursors (radicals or ions) for particle generation and growth in pulsed plasmas, as compared with continuous-wave plasmas. Recently, pulsed plasma discharges have been considered as a relatively simple method to suppress the generation and growth of particles in plasmas and to prepare high-quality thin films by reducing particle contamination at a maximum deposition rate of 15 Å/s.[1,2,7] Watanabe's group[7,8] studied the synthesis of high-quality thin films by reducing the generation of nano-sized particles in pulse-modulated plasmas, and they proposed a mechanism for particle suppression in the pulsed-plasma reactor by using a model considering the diffusion and growth of particles during t_{off} in the monomer-generation region. There have been several experimental studies on particle growth in pulsed-plasma processes, but no theoretical study on particle growth in pulsed-plasmas has been made systematically to understand the particle size distributions during the pulse cycle.

We have developed a discrete-sectional model to analyze particle growth by coagulation between particles in continuous-wave plasma processes.[9] In this study, the discrete-sectional model that we had developed was extended to analyze the particle growth in the pulsed SiH_4 plasma process during plasma-on and -off. We analyzed the evolution of particle size distribution in pulsed plasmas for various pulse frequencies.

Theory

Figure 1 shows the model to analyze the particle growth in pulsed plasmas during t_{on} (a) and t_{off} (b). The plasma reactor proposed by Shiratani et al.[7] was considered as the model reactor. The upper and lower electrodes are designed to have many perforations, so that the gas stream can pass through the electrodes and we can expect plug flow for the gas stream inside this plasma reactor. In the plasma reactor when dense with particles, the particles are dispersed in the bulk plasma region and are believed to grow by coagulation between particles.[9,10] During plasma-on, the plasma reactor is assumed to be a continuously stirred tank reactor because the negatively charged particles are caught inside the bulk

Correspondence concerning this article should be addressed to K.-S. Kim at kkyoseon@kangwon.ac.kr.

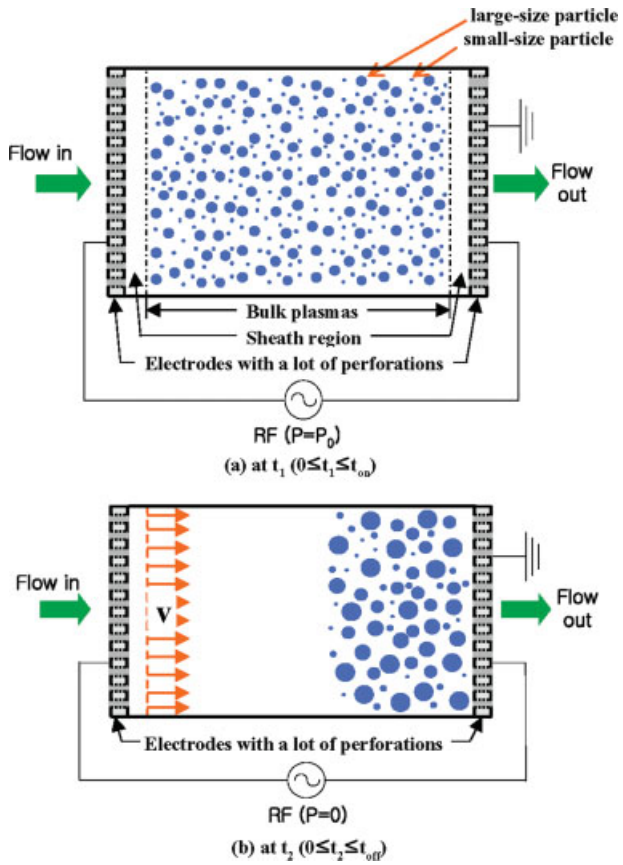

Figure 1. Model of particle growth in dusty plasmas during (a) plasma-on (t_{on}) and (b) plasma-off (t_{off}).

[Color figure can be viewed in the online issue, which is available at www.interscience.wiley.com.]

plasma region by electrostatic repulsion in the sheath regions[9] but, during plasma-off, the plasma reactor is assumed to be a plug flow reactor because the plasma sheath regions collapse away and the particles can flow out of the plasma reactor. To investigate the evolution of the particle size distribution in pulsed plasmas, we applied the volume-conserved discrete-sectional model equations (Eqs. 7–10 in Kim and Kim[9]), considering the effects of fluid flow, particle generation, and particle coagulation in the plasma reactor. The monomers are assumed to be generated only during t_{on}. During t_{on}, the particles can be charged positively or negatively or can be in a neutral state by Matsoukas and Russell,[11] and we can calculate the fractions of particles charged positively or negatively or in a neutral state from the particle charge distribution function and use these to obtain the collision frequencies between particles (Eqs. 11–17 in Kim and Kim[9]). The positively charged and neutral particles pass out of the reactor with the fluid flow, but the negatively charged particles are caught inside the plasma reactor by electrostatic repulsion.[9,10,12,13] During t_{off}, monomers are no longer generated and the concentrations of electrons and positive ions become zero quickly in the plasma reactor; all particles lose their charges to become neutral and can pass out of the reactor by fluid convection. We used the collision frequency function between neutral particles to calculate the particle coagulation rate during t_{off}. In pulsed plasmas, the changes of electron and ion concentrations occur within 10s of μs just after plasma-on or -off.[3,6,14,15] The pulse frequency ranges from 5 to 1000 Hz in this study, corresponding to t_{on} or t_{off} from 0.1 s to 5×10^{-4} s (500 μs) at a duty ratio of 50%; t_{on} or t_{off} is much longer than 10s of μs, and we assumed that the changes of electron and ion concentration just after t_{on} or t_{off} did not significantly affect the particle charging during t_{on} or t_{off}.

The modified discrete-sectional model equations were solved numerically by ODE solver, VODPK subroutine, to predict the particle size distribution in the plasma reactor during t_{on} and t_{off}. During t_{on}, the electron concentration changes with time as the particle concentration and size change in the plasma reactor, and we calculated the electron concentration in every time step of integration by solving the electroneutrality condition; we used this to predict the particle charge distributions. During t_{off}, the plasma reactor is divided into two regions (regions where particles exist and do not exist, respectively) based on the assumption of a plug flow reactor (Figure 1b). In the region where particles exist, the particles will grow by coagulation between neutral particles. The particle concentrations during t_{off} are calculated by multiplying (reactor volume with particles)/(total reactor volume) to take averages for the whole reactor volume.

Results and Discussion

The particle size distributions in pulsed SiH_4 plasmas during plasma-on and -off were analyzed for various process conditions as in Kim and Kim.[9] The size of particle monomer (d_1), residence time (τ_{res}), and duty ratio (D) were 1 nm, 0.1 s, and 50%, respectively. The pulse frequency (f_p) was in the range from 5 to 1000 Hz.

Figure 2 shows the change of particle size distribution with time ($0 < t \leq 0.2$ s) for a pulse frequency of 5 Hz and a duty ratio of 50%. The plasma is on for $0 < t \leq 0.1$ s and off for $0.1 < t \leq 0.2$ s. At the beginning of plasma-on (at $0 < t \leq 0.001$ s), the monomer ($d_1 \sim 1$ nm) concentration becomes high because of the fast monomer generation rate and the concentration of small-size particles (1 nm < particle diameter (d_p) $\leq$2.5 nm) increases quickly because the small-size particles are generated fast by coagulation between smaller particles. At $t = 0.005$ s, large-size particles appear by coagulation between small-size particles and grow for $0.005 \leq t \leq 0.1$ s and, at $t = 0.1$ s, the particle size distribution becomes bimodal with small-size and large-size particles.

During t_{off} ($0.1 < t \leq 0.2$ s), the particles in all size regimes are in a neutral state and they pass out of the reactor with plug fluid flow. The small-size particle concentration decreases quickly, because the monomer generation stops and the small-size particles disappear by fast coagulation with other particles. The large-size particle concentration decreases slowly because large-size particles are still generated by coagulation with small-size particles during t_{off}. At $t = 0.12$, 0.16, and 0.19 s, the particle size distributions become bimodal with small-size and large-size particles, but they have different shapes from those at 0.005, 0.02, and 0.1 s. The large-size particles during t_{on} grow more quickly,

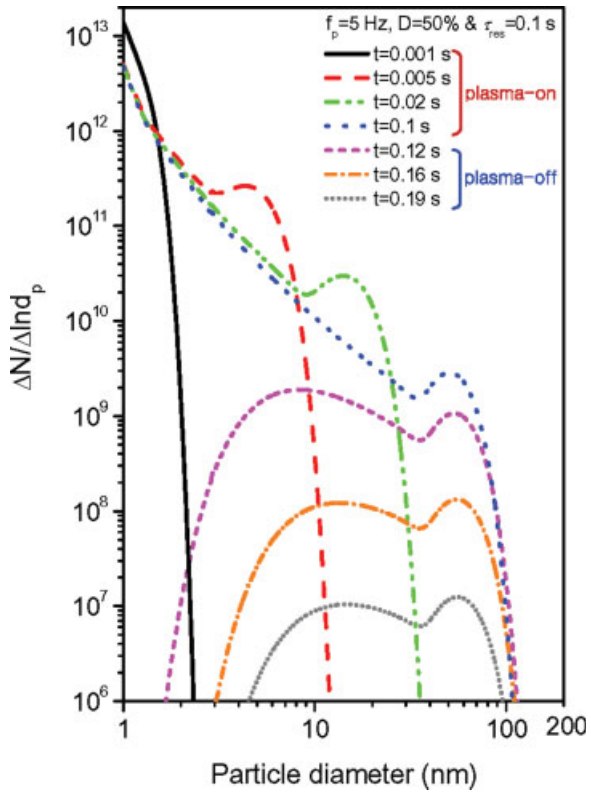

Figure 2. Particle size distributions for various times (d_1 = 1 nm, f_p = 5 Hz, τ_{res} = 0.1 s, D = 50%).

[Color figure can be viewed in the online issue, which is available at www.interscience.wiley.com.]

by faster coagulation with small-size particles, than during t_{off}, because the small-size particle concentration during t_{on} is higher than during t_{off}. At t = 0.2 s, there are no particles remaining inside the reactor, because all particles flow out of the reactor at the end of t_{off} (t_{off} is equal to τ_{res} of 0.1 s) and the particle size distribution in the next pulse cycle is not affected by that in the previous pulse cycle.

Figure 3 shows the change of particle size distribution with time ($0.2 < t \leq 0.3$ s) for a pulse frequency of 10 Hz and a duty ratio of 50% (t_{on} and t_{off} = 0.05 s). The t_{off} here is shorter than τ_{res}, the particles generated in the previous cycle are not swept out of the reactor completely during t_{off}, and the particle size distribution in the next cycle is affected by that in the previous cycle. At t = 0.21 s, we find three modes of particle size distribution: small-size particles ($1 \leq d_p \leq 5$ nm) appearing quickly by fast monomer generation, medium-size particles ($5 \leq d_p \leq 20$ nm) appearing by fast coagulation between small-size particles of high concentration, and large-size particles ($20 \leq d_p \leq 100$ nm) left over from the previous pulse cycle. The medium-size particles continue to grow by coagulation with small-size particles ($0.21 \leq t \leq 0.25$ s) and, at t = 0.25 s, the medium-size particles are almost merged with the large-size particles and the particle size distribution finally becomes bimodal with small-size and large-size particles.

During t_{off} ($0.25 < t \leq 0.3$ s), the particle concentration decreases with time because of particle coagulation, fluid flow and absence of particle generation. The small-size particle concentration decreases quickly by fast coagulation with other particles, and the large-size particle concentration decreases slowly because some large-size particles continue to be generated by coagulation between smaller particles during t_{off}. In Figure 3, t_{off} is too short for all particles to flow out of the plasma reactor by fluid convection and particles still remain inside the plasma reactor at the end of plasma-off (t = 0.3 s). The particle size distribution at t = 0.3 s, which is bimodal with small-size and large-size particles, becomes the initial condition to calculate the particle size distribution in the next cycle, and we find large-size particles from the beginning of plasma-on.

The particle size distributions at the end of plasma-on and -off are presented in Figure 4 for various pulse frequencies. For pulse frequencies of 10, 50, and 100 Hz, t_{on} and t_{off} are 0.05, 0.01, and 0.005 s, respectively, for a given duty ratio of 50%, and the end of plasma-on is 0.25, 0.29, and 0.295 s, respectively, but the end of plasma-off is 0.3 s for all three frequencies. At the end of plasma-off, particles still remain inside the plasma reactor, because t_{off} is shorter than τ_{res}. As the pulse frequency decreases, new monomer generation takes a longer time during t_{on} in each pulse cycle and the large-size particles become larger at the end of t_{on}. During t_{off}, new monomers are not generated and the particle concentration decreases by coagulation between particles and fluid convection. As the pulse frequency decreases, the particle

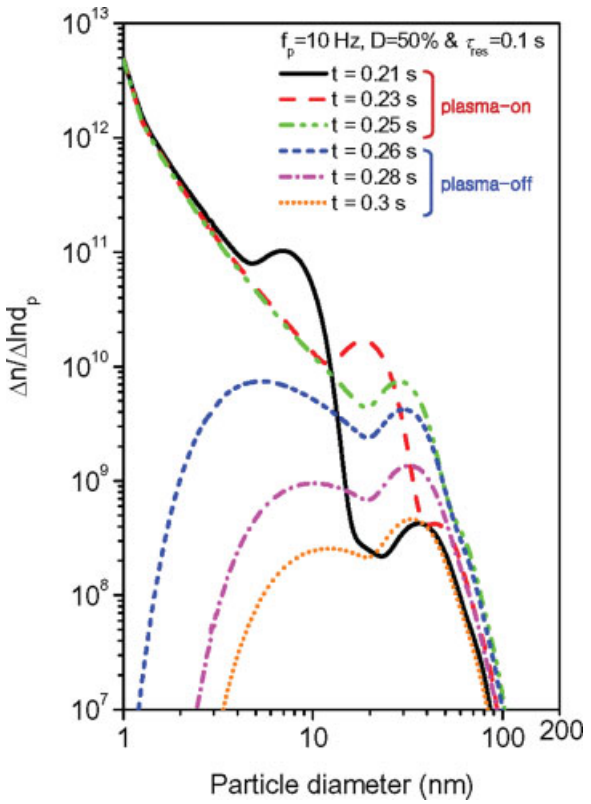

Figure 3. Particle size distributions for various times (d_1 = 1 nm, f_p = 10 Hz, τ_{res} = 0.1 s, D = 50%).

[Color figure can be viewed in the online issue, which is available at www.interscience.wiley.com.]

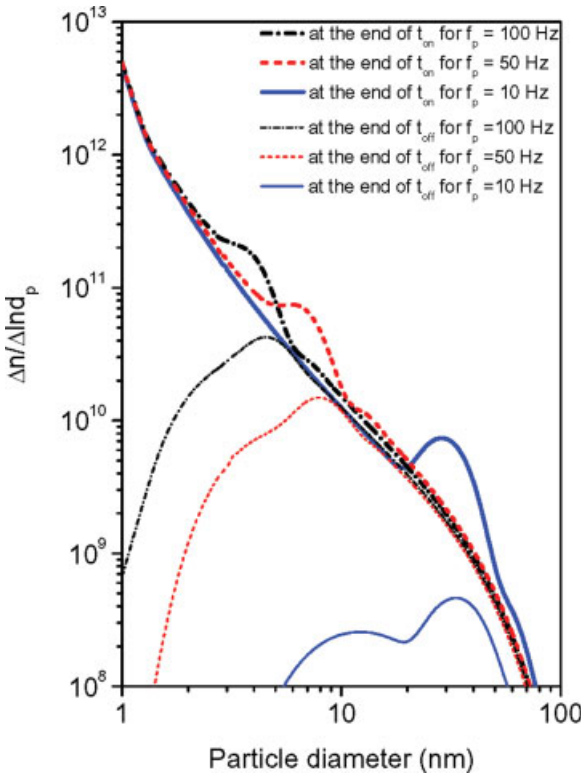

Figure 4. Particle size distributions at the end of plasma-on and -off for various pulse frequencies (d_1 = 1 nm, τ_{res} = 0.1 s, D = 50%).

[Color figure can be viewed in the online issue, which is available at www.interscience.wiley.com.]

concentration at the end of t_{off} decreases because particle coagulation and fluid convection have taken place for a longer time. In continuous-wave plasmas, the particle size distribution in the plasma reactor becomes clearly bimodal with small-size and large-size particles and the mode of large-size particles becomes quite narrow.[9,12,13] In pulsed plasmas, the particle size distribution changes with time during the cycle and there is no clear difference in particle size distribution between the two size modes, as compared with that in continuous-wave plasmas. The large-size particles in pulsed plasmas become smaller than those in continuous-wave plasmas because the pulse modulation prevents the growth of large-size particles in pulsed plasmas.

Figure 5 shows the mean particle diameters in continuous-wave and pulsed plasmas for various pulse frequencies by experiment[7] and by a numerical method in this study for the same process conditions. In their experiments, after plasma-off, the particles are redistributed inside the plasma reactor by particle diffusion and the diameter of the particles is determined from their diffusivity measured by a photocounting laser-light-scattering method. The predicted mean particle diameter was obtained from the particle size distribution at $0.2t_{off}$ after plasma-off by averaging the particles in all size regimes. In pulsed plasmas, the mean particle diameter becomes smaller than that in continuous-wave plasmas because the number of monomer particles generated during t_{on} is smaller than that in continuous wave plasmas and also particles flow out of the reactor during t_{off}. As the pulse frequency in pulsed plasmas increases, the large-size particles at the end of t_{on} become smaller because of the reduced monomer generation and shorter coagulation time during t_{on} and, as a result, the mean particle diameter decreases. The model results were in good agreement with the published experimental data.[7] The results by experiment and those by the numerical method prove that the particle generation and growth in the SiH_4 PCVD process can be suppressed by the pulsed plasma method, which is important in preparing high-quality thin films in the SiH_4 PCVD process. Shiratani et al.[7] also showed that the changes of particle concentration for various pulse frequencies and particle concentrations in their experiments were in the range of 5×10^8 to 1.4×10^{10} #/cm^3, but their experimental results do not show a clear relationship between particle concentration and pulse frequency. The particle concentrations predicted by our model for the same process conditions are in the range of 1.2×10^{10} to 2.9×10^{10} #/cm^3.

Conclusions

We analyzed particle growth in pulsed SiH_4 plasmas during plasma-on and -off by applying a discrete-sectional model[9] and investigated the effects of pulse frequency on

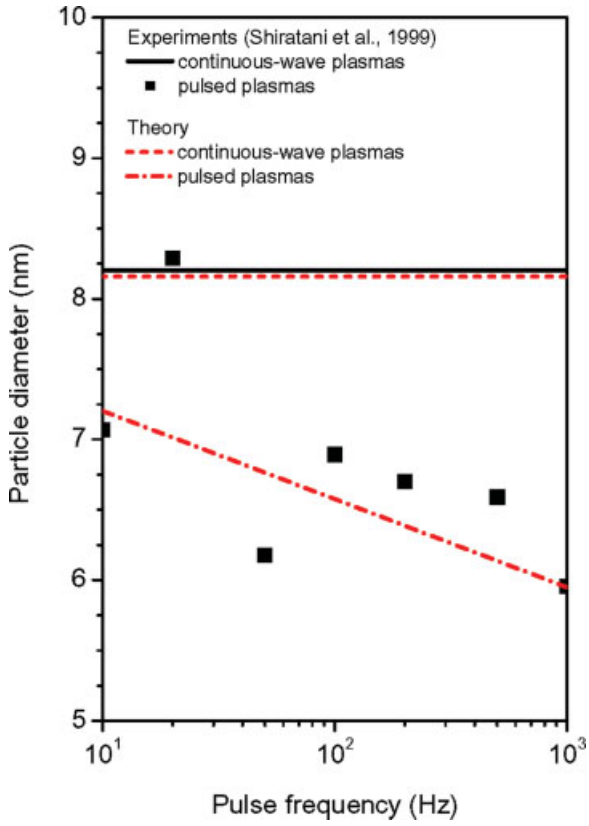

Figure 5. Mean particle diameters in continuous-wave and pulsed plasmas for various pulse frequencies by experiments[7] and by the numerical method in this study for the same process conditions.

[Color figure can be viewed in the online issue, which is available at www.interscience.wiley.com.]

particle growth. During plasma-on, the plasma reactor was assumed to be a continuously stirred tank reactor but, during plasma-off, it was assumed to be a plug flow reactor. At the beginning of plasma-on, there is a high concentration of small-size particles and, later, large-size particles appear and grow by particle coagulation. During plasma-off, monomer generation stops and the particle concentration decreases with time by the effects of particle coagulation and fluid flow. For t_{off} longer than the residence time, the particle size distribution in pulsed plasmas becomes bimodal with small-size and large-size particles, whilst, for t_{off} shorter than the residence time, it becomes trimodal with small-size, medium-size, and large-size particles at the center of t_{on}, because the large-size particles formed in the previous cycle still remain inside the plasma reactor during t_{off} and these affect the particle size distribution in the next cycle. As the pulse frequency decreases, more monomer particles are generated during the longer plasma-on time and the large-size particles become larger at the end of t_{on}. This study shows that the pulsed-plasma process can be used to suppress particle growth in the SiH_4 plasma process and can be a good method to prepare high-quality thin films by reducing particle contamination.

Acknowledgments

This research was performed for the Hydrogen Energy R&D Center, one of the 21st Century Frontier R&D Programs, funded by the Ministry of Science and Technology of Korea.

Literature Cited

1. Madan A, Morrison S. High deposition rate amorphous and polycrystalline silicon materials using the pulsed plasma and hot-wire CVD technique. *Sol Energy Mater Sol Cells*. 1998;55:127–139.
2. Licheng MH, Timmons RB, Lee WW, Chen Y, Hu Z. Pulsed plasma polymerization of pentafluorostyrene: synthesis of low dielectric constant films. *J Appl Phys*. 1998;84:439–444.
3. Anders A. Fundamentals of pulsed plasmas for materials processing. *Surf Coat Technol*. 2004;183:301–311.
4. Courteille C, Dorier J-L, Hollenstein Ch, Sansonnens L, Howling AA. Partial-depth modulation study of anions and neutrals in low-pressure silane plasmas. *Plasma Sources Sci Technol*. 1996;5:210–215.
5. Howling AA, Sansonnens L, Dorier J-L, Hollenstein Ch. Time-resolved measurements of highly polymerized negative ions in radio frequency silane plasma deposition experiments. *J Appl Phys*. 1994; 75:1340–1353.
6. Kushner MJ. A model for the discharge kinetics and plasma chemistry during plasma enhanced chemical vapor deposition of amorphous silicon. *J Appl Phys*. 1988;63:2532–2551.
7. Shiratani M, Fukuzawa T, Watanabe Y. Particle growth kinetics in silane RF discharges. *Jpn J Appl Phys*. 1999;38:4542–4549.
8. Watanabe Y, Shiratani M, Koga K. Nucleation and subsequent growth of clusters in reactive plasmas. *Plasma Sources Sci Technol*. 2002;11:A229–A233.
9. Kim D-J, Kim K-S. Analysis on nanoparticle growth by coagulation in silane plasma reactor. *AIChE J*. 2002;48:2499–2509.
10. Kim K-S, Kim D-J. Modeling of rapid particle growth by coagulation in silane plasma reactor. *J Appl Phys*. 2000;87:2691–2699.
11. Matsoukas T, Russell M. Particle charging in low-pressure plasmas. *J Appl Phys*. 1995;77:4285–4292.
12. Kim D-J, Kim K-S, Zhao Q-Q. Production of monodisperse nanoparticles and application of discrete-monodisperse model in plasma reactors. *J Nanoparticle Res*. 2003;5:211–223.
13. Kim K-S, Kim D-J, Yoon JH, Park JY, Watanabe Y, Shiratani M. The changes in particle charge distribution during rapid growth of particles in the plasma reactor. *J Colloid Interface Sci*. 2003;257: 195–207.
14. Ashida S, Lieberman MA. Spatially averaged (global) model of time modulated high density chlorine plasmas. *Jpn J Appl Phys*. 1997; 36:854–861.
15. Ramamurthi B, Economou DJ. Two-dimensional pulsed-plasma simulation of a chlorine discharge. *J Vac Sci Technol A*. 2002;20:467–478.

Manuscript received Sept. 21, 2007, revision received Apr. 9 2008, and final revision received Jun. 13, 2008.